

HEAT TRANSFER ENHANCEMENT AND PRESSURE DROP FROM TUBE BANK WITH SPLITTER PLATES IN CROSS-FLOW EMPLOYING RANS AND LES TURBULENCE MODELS

by

**Mohamed A. KARALI^{a*}, Bandar Awadh ALMOHAMMADI^b,
Rayed S. ALSHAREEF^c, Ahmed GAD^b, Hassanein A. REFAEY^{b,d*},
and Khaled ZIED^{b,e}**

^aDepartment of Mechanical Engineering, Faculty of Engineering and Technology,
Future University in Egypt, New Cairo, Egypt

^bDepartment of Mechanical Engineering, College of Engineering at Yanbu,
Taibah University, Yanbu Al-Bahr, Saudi Arabia

^cDepartment of Chemical Engineering, College of Engineering at Yanbu,
Taibah University, Yanbu Al-Bahr, Saudi Arabia

^dDepartment of Mechanical Engineering, Faculty of Engineering at Shoubra,
Benha University, Cairo, Egypt

^eMechanical Design Engineering Department, Faculty of Engineering EL-Mattaria,
Helwan University, Cairo, Egypt

Original scientific paper

<https://doi.org/10.2298/TSCI241209026K>

Heat transfer enhancement from tube bank in cross-flow with air can be achieved for energy saving by enhancing the flow turbulence nature. Adding splitter plates to the tubes' trailing edges, besides, increasing the heat transfer surface's roughness are proposed options to enhance the flow turbulence. However, few literatures are available to discuss this, moreover, almost all available CFD models employ RANS turbulence models and away from using large eddy simulation (LES). Accordingly, this work was presented to compare the employing of RANS and LES turbulence models for such problems at low Reynolds numbers. Toward this objective, a complete 3-D CFD model consisting of seven rows of tubes in flow direction is developed without using any symmetrical boundary conditions. The present study includes the impact of the Re_{max} range (500-4500), for three surface relative roughnesses: k_s/D of 0, 0.01, and 0.02. The local turbulence and heat transfer characteristics are discussed. The findings confirmed that the two proposed options for heat transfer enhancement succeeded in doubling it. The LES is superior to RANS models in resolving a wide spectrum scale of flow eddies. The results are useful in designing more efficient heat exchangers, especially at low Reynolds number.

Key words: heat transfer, tube bank, RANS, LES, pressure drop

Introduction

The design of energy-efficient systems is essentially required for the energy-saving goals [1-4]. In engineering practice, cross-flow over tube banks is frequently encountered in heat transfer apparatus such as steam generation in a furnace, condensers, and evaporators in refrigerators, power plants, air conditioners, and heat recovery systems. The flow of cross-flow over a tube bank is characterized to be turbulent. As the pressure drops, the heat transfer coeffi-

* Corresponding authors, e-mail: mohamedkarali@yahoo.com, hassanein.refaey@feng.bu.edu.eg

cient, h , for the tubes in the following rows rises because the first-row tubes act as a turbulence grid. However, the heat transmission coefficient stabilizes after the fourth or fifth row [5, 6]. Its uneven distribution results in changing turbulent movements which can carry momentum, heat, and mass. These movements have a noteworthy impact on flow field velocity, temperature, and pressure distribution. The turbulent movements profile is 3-D, unstable, and unsuitable medium, in which they are different from enormous eddy sizes, which correspond to low frequency fluctuations. Trivial eddies where dissipation occurs, correspond to high frequency oscillations, the turbulent movements characterized by eddies of various sizes.

Therefore, two crucial aspects for researching turbulence are choosing the turbulence technique rather than the model, and the fact that 3-D simulation is still the best way to explain such complicated flows. The turbulence technique should provide models *whose predictions are close to those of the equations* but are computationally easier than the Navier-Stokes equations. The first method statistically averages the Navier-Stokes equations which are known as RANS. The LES is the second method. For the Navier-Stokes equations, LES uses a spatial averaging filter to recover large-scale velocity, pressure, and temperature structures and reduce their small-scale features. After modelling tiny-scale effects on enormous sizes only big-scale random motion is resolved. The third method, direct numerical simulation (DNS), solves Navier-Stokes equations without turbulence. The complete spectrum of turbulence's spatial and temporal scales, from the lowest dissipative scales (Kolmogorov scales) to the integral scale, which is associated with the movements that contain most of the kinetic energy must be resolved. The DNS is necessary for investigating complicated flow phenomena that need a lot of computer resources, but not for engineering calculations. The LES outperforms RANS when large-scale features dominate flow behavior and unstable phenomena such as vortex shedding occur, particularly at lower Reynolds numbers. Though cheaper than DNS, LES calculations are expensive [7].

Many research efforts are devoted to enhancing the turbulence within cross-flow over tube banks while keeping an eye on the pressure drop. The splitter plates (SP) may be positioned at the dragging edge of the tubes of a cross-flow heat exchanger to improve heat transmission. Due to their role as enlarged heat transfer surfaces and their ability to minimize pressure drop in cross-flow heat exchangers via the suppression of vortex shedding, the inclusion of such SP significantly improves heat transfer [8]. Apelt *et al.* [9], pointed out that adding SP to circular cylinders reduces drag independent of the Reynolds number. A CFD analysis was presented by Kwon and Choi, [10] to examine the effect of SP length on vortex shedding. Furthermore, the SP critical length required to completely stop the shedding was identified. The square cylinder was the subject of another CFD investigation by Park [11], and the findings showed that the shorter SP was responsible for controlling the cylinder's downstream wake. The impact of putting SP in a staggered tube bank in cross-flow with air, which consists of five rows of tubes in the flow direction, was exposed to experimental and CFD studies by Mangrulkar *et al.* [12]. They employed the RANS technique and suggested utilizing the RNG $k-\epsilon$ turbulence model with such flow issues for SP with a tube length-to-tube diameter ratio of one. The examined range of Re_{max} was 5500-14500. The findings demonstrated that the SP facility boosted the fluid-flow's Nusselt number while decreasing pressure drop. Later, Mangrulkar *et al.* [13], published further research utilizing six rows of tubes arranged in the flow direction examine various SP geometries. It was discovered that for the majority of patterns, the SP with the geometrical parameters, $L/D = 1.0$ and $t/D = 0.20$ improved the Nusselt number and decreased the overall pressure drop. The work of Mangrulkar *et al.* [12], was quantitatively enlarged by Elmekawy *et al.* [14], to add to the optimization of the SP thickness. The RANS RNG $k-\epsilon$ turbulence model was also used. According to their findings, the SP should be thin to maintain the best heat exchanger performance.

Another proposed option for heat transfer augmentation is by roughing the associated surfaces, as this will increase turbulence. The surface roughness can be expressed as either the surface relative roughness, k_s/D , or the surface roughness height, k_s . The D is the outer diameter of the tube, and k_s [mm] is the comparable roughness height of sand particles [15]. The roughness conditions determine both the crucial Reynolds number and the drag coefficient. The literature introduces numerous surface roughening techniques. Various approaches such as sandpaper [16-18], sand grain [19], arrays of rods [20, 21], and regular configurations of pyramids [22-25] have been widely used. Different work such as that presented in [16, 20, 21, 22, 23, 25, 15], and computer-based studies [26-30] have looked at how roughness affects the thermal boundary-layer and, the value of heat transfer coefficient, h , which represents the air-flow around a cylinder in a circle. However, researchers use existing computational studies to explore the impact of roughness on a single cylinder in cross-flow to air. You may find further studies on the impact of roughness on pressure drops, velocity vectors, and lift and drag coefficients in Taylor *et al.* [31]. Here are detailed summaries of related work. Achenbach [16], Achenbach [22], and Achenbach and Heinecke [23] carried out numerous experiments to ascertain the impact of surface roughness on h and flow topology surrounding a circular cylinder. Achenbach [16] reported using the two-roughness approach, which involves warping sandpaper around the cylinder. Achenbach [22], and Achenbach and Heinecke [23], used regular pyramid lay-outs. The relative roughness (k_s/D) ranged between $1.1 \cdot 10^{-3}$ and $9.0 \cdot 10^{-3}$. Tetsu *et al.* [25] analyzed the local h and boundary-layer temperature trends to determine how roughness affects natural-convection for water flow through a vertical cylinder. Their results suggested that the roughness of the water's surface enhanced the rate of local heat transmission. The impact of k_s/D on the parameter h is the subject of studies [20, 24]. Kolar [24], claimed that rising tube roughness lowered the mean velocity, improved the friction factor, and decreased the value of h .

Al-Rubaiy [15], reviewed the literature to determine the unique and typical influences of the ratio, (k_s/D). This ratio was modified from 0-0.00725 and the turbulence intensity varied from 2.2%-9.7%. Results established that surface roughness was necessary to improve the thermal performance. Arenales *et al.* [18], investigated how surface roughness affected copper tubes in boiling water between 0.032 m and 0.544 m. The discoveries showed that rough tubes increase the value of h by 1.5 times more than smooth ones. The incompressible flow through a rounded cylinder with ($k_s/D = 0.5\%$) was quantitatively examined by Kawamura and Takami, [26]. No turbulence model was used and the Reynolds values varied from 1000-100000. At around $Re = 20000$, the drag coefficient significantly decreased. This demonstrated that the crucial Reynolds number had been captured within their computational bounds. Our research team in Karali *et al.* [32] presented a CFD analysis on the influence of surface roughness on heat transfer and pressure decrease in a staggered tube bank in cross-flow using air. This study benefits from a complete 3-D CFD model without symmetrical boundary conditions. The tube bank has five rows of tubes facing air-flow. The enlarged analysis includes Re_{max} changes between 5000 and 100000. The $k_s/D = 0$ (smooth), 0.01 (rough), and 0.02 (rough). As suggested by earlier studies: using the RANS RNG $k-\epsilon$ turbulence model [12, 13]. The conclusions displayed that heat transfer surface roughness promotes heat transfer, and pressure drop increases somewhat. Improving surface roughness and including SP doubled the heat transfer rate.

Regarding the use of LES turbulence models, there are limited CFD works from the literature that employ LES models for cross-flow over a single cylinder, rather than for cross-flow over virtually non-existent tube banks [33-39]. The following are some of these researches. Breuer [33], numerically studied the turbulent flow past a circular cylinder at $Re = 3900$ using LES. The objective was to investigate numerical and modelling factors that affect the LES solution quality. Investigations were done into five separate schemes. No-slip boundary

circumstances were utilized at solid walls due to the study's being limited to low Reynolds numbers. There are two separate subgrid-scale models are employed. The LES calculations without subgrid-scale modelling were also done to illustrate the models' efficiency. The obtained results were compared to the experimental data for verification purposes. Rodi [34] presented using DNS. The large-scale eddy flow LES was flowing in a low pressure turbine cascade with wakes routinely traveling down the cascade channel. The studied flow was through a surface-mounted rounded cylinder with a 2.5 height-to-diameter ratio. The results showed that DNS and LES can reliably predict engineering-relevant turbulent flows despite their high cost. In situations of unsteadiness, such as shedding, and large-scale structures, DNS is better than RANS techniques, and DNS has become a significant instrument for transition process study. The LES was used by Sarkar [35] to study flow through a cylinder near a wall. To understand flow physics' insights into boundary-layer-wake exchanges for three gap-to-diameter ratios. The current LES shows the shear layer's instability and the growth of small-scale eddies. The CFD analysis was utilized by Afgan *et al.* [36] to study cross-flow over two heated infinite cylinders in an in-line arrangement. Using the dynamic Smagorinsky's non-isothermal LES model dependent on the cylinder diameter and free stream velocity, at a Reynolds number of 3000. Two distinct Prandtl number values, $Pr = 0.1$ and 1.0 were examined with a cylinder gap ratio of $1.0 < L/D < 5.0$. The upstream cylinder's average Nusselt number was discovered to be greater than the downstream one, which is their key discovery. Additionally, it was discovered that the maximal Nusselt number is independent of the spacing ratio and is situated at the separation angle.

From the preceding discussions, it can be concluded that only a limited number of CFD models from the literature address the combined effects of surface roughness in tube banks in cross-flow with air and the addition of SP on heat transfer and pressure drop at low Reynolds numbers. Additionally, implementing full 3-D simulations without applying symmetrical boundary conditions provides greater detail and aligns the simulation results more closely with experimental findings by modelling the problem as it occurs in practice. In the long run, this approach reduces the need for challenging experimental work. Moreover, almost no work has been found in the literature to discuss the same topic using LES turbulence models due to the highly intensive computational resources needed.

This paper aims to compare the performance of RANS and LES turbulence models in addressing challenges associated with low Reynolds number applications. The study seeks to provide deeper insights into the turbulent behavior of such problems. Another major focus of the study is to examine the local turbulence and heat transfer characteristics in detail. To achieve this, the number of stream-wise tubes increased to seven. These critical considerations underscore the significance of the present study, which contributes to the design of more efficient heat exchangers, particularly for low Reynolds number conditions.

Numerical simulations

Geometric configuration

The numerical simulation for a staggered tube bank in cross-flow using air will be employed for this investigation. It comprises six half-dummy tubes to maintain the flow characteristics inside the arrangement, along with 18 thermally heated tubes. The transverse columns are three in a staggered lay-out, with seven rows in the streamwise direction. The used dimensions are found in Incropera *et al.* [5], which may be used with numerous devices, $D = 16.4$ mm, 34.3 mm is the longitudinal pitch, 31.3 mm is the transverse pitch, and 37.7 mm is the diagonal pitch. The duct height ($H = 95.4$ mm) is based on the previously mentioned measure-

ments. The spanwise tube length is assumed to be 190.8 mm ($W/H = 2$), and W is duct width. The 18 rectangular SP are secured to each tube's trailing edge in the case of SP. The SP length is ($L_{SP} = D$) and their thickness is assumed to be 1.75 mm. The initial tube row is $2D$ away, and the final tube row is assumed to be $14D$ away from the end of the CFD domain. The ANSYS design modeler R18.0's numerical simulation for the case of SP is shown in fig. 1 with all geometrical parameters.

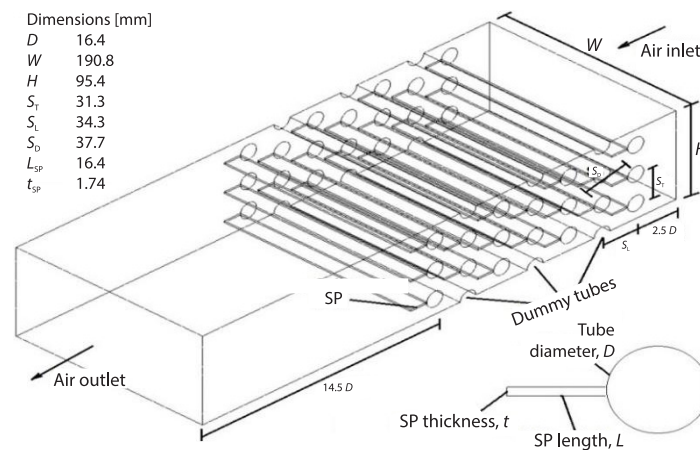


Figure 1. Geometrical configuration for the case of SP, showing the seven tube rows in a streamwise direction

Meshing properties

The ANSYS-ICEM Mesh R18.0 meshes the discretized solution domain with a fine mesh adjacent to all solid surfaces in the boundary-layer regions and areas with significant gradients of the dependent variables. This method inflates such areas using 18 layers with a 1st layer of 0.08 mm thickness including 1.1 inflation rate. This guaranteed lower Y^+ values for all situations examined. In the case of SP, fig. 2 depicts the produced mesh in fig. 2(a) an overall view and fig. 2(b) a zoomed-in sight to highlight the inflating layers for both air and SP domains. Another concern for creating the mesh sometimes referred to as *mesh independence* is whether there are enough nodes and if the iterative solution procedure has workable convergence criteria. In the smooth case with SP at $Re_{max} = 2500$, several meshes were used to demonstrate mesh independence. Additionally, the matching average Nusselt number values were compared (to be explained later). The respective meshes carry different cell sizes for the air domain and the SP domain with 3.06 (5, 0.4 mm), 4.5 (4, 0.35 mm), 6.4 (5, 0.3 mm), 6.6 (4, 0.3 mm), 7.3 (3, 0.3 mm), and 8.9 (2, 0.3 mm) million counted for the total number of nodes. It was deter-

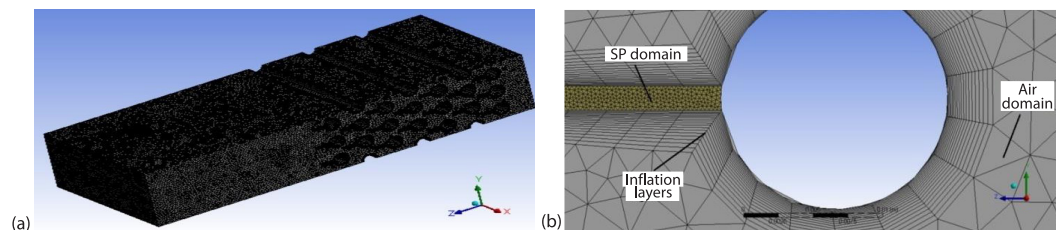


Figure 2. Mesh properties (Ansys-ICEM R18.0); (a) overall view showing seven tube rows and (b) zoom-in view

mined that any number of nodes more than one of 6.6 million will provide very little marginal difference in Nusselt number. The mesh with 7.3 million nodes was chosen throughout the whole study to provide a better understanding of the intricate structure of turbulence.

Methodology

The RANS and LES methodologies were employed in this study, using the ANSYS CFX R18.0 numerical tool. The discretization of limited volumes underlies this piece of software. Two domains may be distinguished in the case of tubes containing SP: air-based fluid domain, and aluminum-based solid domain. The hot tube surface is described as no-slip walls with defined roughness which varies from: $k_s/D = 0$ (smooth), to $k_s/D = 0.02$ [15, 18, 26, 32], and at a fixed surface temperature of 363 K. The SP bases are also kept at 363 K and have the same surface roughness as the tube walls. While adiabatic wall boundary conditions refer to all other walls. The moving fluid intake velocity is calculated based on Re_{max} values of 500, 1500, 2500, 3500, and 4500 [32, 36]. The air inlet temperature is 288 K. For all studied cases the RNG $k-\varepsilon$ turbulence model is applied as it was recommended by other investigators [12, 14, 32, 40-44] to be the best RANS model that describes the current problem. While the LES turbulence model is tested for six cases namely: without SP and $k_s/D = 0.01$ for Re_{max} of 2500 and 4500, without SP and $k_s/D = 0.02$ for Re_{max} of 500 and 4500, and with SP and $k_s/D = 0.01$ for Re_{max} of 3500, and rough ($k_s/D = 0.02$) for Re_{max} of 4500. However, an initial test was conducted to check the flow type for the lowest $Re_{max} = 500$. Therefore, the laminar model was checked beside the RNG $k-\varepsilon$, and results from the two models were compared particularly based on the average Nusselt number, where the same methodology was used by Gorman *et al.* [45]. It was noted that there is a deviation of about 1% between the results from the two models, which indicates that the turbulent flow type is prevailing even for the lowest $Re_{max} = 500$. This can be attributed to the flow nature of such problem configuration with a staggered tube bank.

A residual mean square of 10^{-6} and below was chosen as the primary solution convergence criteria for both techniques, RANS and LES. For the LES model, convergent statistics are ensured by simulating the instances for a significant time. The best convergence was evaluated during the first transient period. Statistics were typically gathered during intervals of roughly $100 D/V_\infty$ time units. With a Courant number setting between 0.5 and 1, the number of loop iterations every shedding cycle is maintained at 10. The solution was operated on an Intel (R) Xeon (R) CPU E5-26700 at 2.6×2 GHZ 16 cores 32 GB RAM system in parallel local MPI.

For incompressible, single-phase, fully developed flow, the RANS RNG $k-\varepsilon$ turbulence model, which incorporates the fundamental mass, momentum, and energy transfer equations, is presented in detail in Wilcox [7], Stefanidis *et al.* [46], and Karali *et al.* [32].

The mass and momentum equations of the LES for incompressible flow are expressed [7, 35, 36]:

$$\frac{\partial \bar{u}_i}{\partial x_i} = 0 \quad (1)$$

$$\frac{\partial \bar{u}_i}{\partial t} + \frac{\partial}{\partial x_j} (\bar{u}_i \bar{u}_j) = -\frac{1}{\rho} \frac{\partial p}{\partial x_i} + \frac{1}{Re} \nabla^2 \bar{u}_i - \frac{\partial \tau_{ij}}{\partial x_j} \quad (2)$$

where \bar{u}_i is the velocity field and $\tau_{ij} = \bar{u}_i \bar{u}_j - \bar{u}_i \bar{u}_j$ – the residual stress tensor that is identified also as the subgrid-scale stress. The inducement of subgrid movements is included in the resolved LES using the model developed by Germano *et al.* [47] and altered by Lilly [48].

Governing equations

The maximum fluid velocity across the tube bank is shown [49, 50]:

$$V_{\max} = \left(\frac{S_T}{S_T - D} \right) V_{\infty} \quad \text{at } S_D > \frac{S_T + D}{2} \quad (3)$$

where D is the tube diameter and S_T and S_D are the tubebank's transversal pitch and diagonal pitch, respectively.

Equation (4) allows for the computation of the Re_{\max} based on V_{\max} :

$$Re_{\max} = \frac{\rho V_{\max} D}{\mu} \quad (4)$$

where ρ and μ are the corresponds to fluid density and dynamic viscosity coefficient, respectively.

Using eq. (5), it is likely to determine the air side total heat transfer rate, Q_a :

$$Q_a = \dot{m}_a c_p (T_{a,o} - T_{a,i}) \quad (5)$$

where \dot{m}_a is the air mass-flow rate, computed after eq. (6), c_p – the air-specific heat, $T_{a,o}$ – the outlet air temperature (evaluated from CFD findings), and $T_{a,i}$ [288 K] – the inlet air temperature:

$$\dot{m}_a = \rho H W V_{\infty} \quad (6)$$

where H and W are the air duct height and width. Thus, the h_{avg} is described:

$$h_{\text{avg}} = \frac{Q_a}{A_s LMTD} \quad (7)$$

where A_s is the total heat transfer surface area, and $LMTD$ is computed:

$$LMTD = \frac{(T_s - T_{a,i}) - (T_s - T_{a,o})}{\ln \left[\frac{(T_s - T_{a,i})}{(T_s - T_{a,o})} \right]} \quad (8)$$

where T_s [363 K] is the hot surface temperature and Nu_{avg} – the attained from:

$$Nu_{\text{avg}} = \frac{h_{\text{avg}} D}{K} \quad (9)$$

where K is the corresponds to the air thermal conductivity.

One main point of interest to discuss here is obtaining the fluid properties, as it essentially influences the calculated results. The air properties are obtained using the CFX library at an air entry of 288 K. And then it was fed to the calculation equations under the assumption that the effects of changes in air temperature throughout the tube bank on air characteristics are insignificant [51, 52].

The total air pressure drop might be established:

$$\Delta p = p_{a,i} - p_{a,o} \quad (10)$$

where $p_{a,i}$ and $p_{a,o}$ are the air static pressures at the inlet and outflow, respectively.

Model validation with experimental work

As previously highlighted, the literature contains a limited umber of experimental studies related to the current research issue. It is also restricted to discussing the feasibility

of incorporating SP at the trailing margins of a tube bank in cross-flow using air-flow. Mangrulkar *et al.* [12] conducted experimental research in an open-channel wind tunnel. Their test rig facility has a rectangular air duct measuring 600 mm in length and $175 \text{ mm}^2 \times 150 \text{ mm}^2$ in cross-section. The test portion consists of 13 examination tubes and four half-blank tubes organized in five rows with a staggered arrangement. A comparable test section is available for circular cylinders fitted with SP. The provided working fluid, air, is introduced at 300 K. The longitudinal and transverse pitch ratios are consistently maintained at 1.75 and 2.0, respectively, for both arrangements. The range of Reynolds number chosen spans from 5500-14500. A SP length ($L_{SP} = D$) is used. Consequently, the existing numerical model delineated in this research for smooth tubes is corroborated by the experimental findings of Mangrulkar *et al.* [12], with the results shown in fig. 3. As noticed in fig. 3, the validation performed throughout the whole range of investigated Re_{max} is reliable with the increasing pattern seen in the experimental findings.

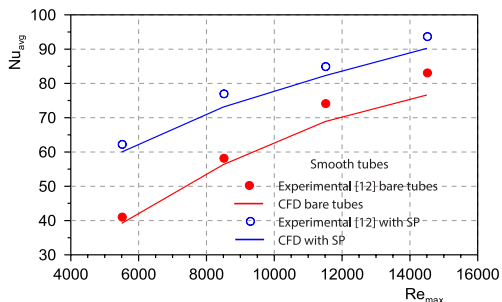


Figure 3. The CFD validation with experimental work for the baseline case (smooth tubes)

Results

Comparison between RANS and LES models

The main finding from this research is comparing the employing of the LES turbulence model with the RANS turbulence model within cross-flow over a staggered tube bank problem. Comparison based on the iso-surfaces of immediate streamwise vorticity colored by the velocity magnitude for the case of with SP and $k_s/D = 0.01$ at $Re_{max} = 3500$ is conducted between using LES, as shown in fig. 4, and RANS, as shown in fig. 5. For the two figures, three sub-images are drawn: fig. 5(a) spanwise view, fig 5(b) zoom-in view, and fig. 5(c) streamwise view. The comparison between figs. 4(a) and 5(a) shows the effectiveness of the LES model in resolving a broad spectrum of eddies over the RANS model. This can be confirmed by the excessively detailed flow vortices found in fig. 4 rather than that found in fig. 5 at the same vorticity level (± 0.01). However, the high computational resources needed are the main obstacles to using such an LES model in real-world applications.

In the prescribed issue with SP, the flow topology is characterized by stagnation patterns in front of the tubes due to the upstream flow striking with the first row of tubes, figs. 4 and 5. The flow then approaches the tube walls. Due to the curvature of the tube circumference, the separation then becomes pronounced, and a vortex region forms behind the tubes. In contrast, installing SP precludes vortex interference from the upper and lower tube sides in the downstream region compared to the absence of SP. The two flow reattaching the SP surfaces from the sides of adjacent tubes to one another. Compared to tubes without SP, stratified flow with weaker vortex strength is produced by tubes with SP. This would reduce the total pressure decline and energy losses in the tube bank. Such flow topologies for different cases; with and without installing SP are similar to limited works from the [12, 14, 32, 34-36, 53]. While the focus difference observed when comparing figs. 4(c) to 5(c), is the flow wake nature after the last row (7th row). The flow wakes vortex region for the LES is shorter in length than found by the one using the RANS model and closer to the tubes trailing edges of the last row. Indeed the shorter vortex length can be appropriate for the physical predictions of such problems. Howev-

er, a comparison based on the resulting actual amounts of heat transfer would be useful for more clarification of using the two models (see coming sections).

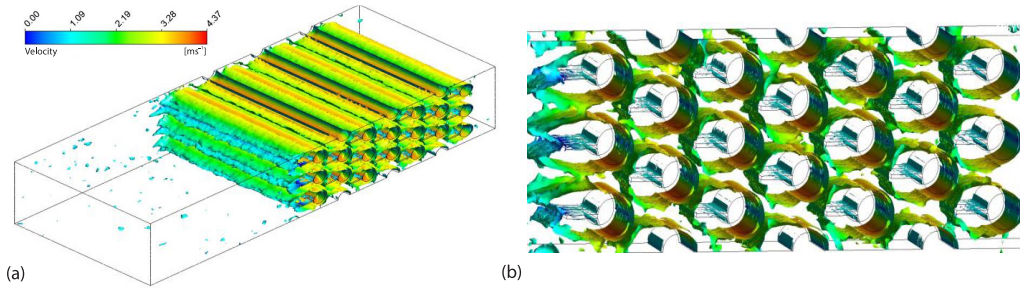


Figure 4. Isosurfaces of instantaneous streamwise vorticity (± 0.01) highlighted by velocity magnitude for the case of with SP rough 0.01 LES $Re_{max} = 3500$; (a) spanwise view, (b) zoom in view, and (c) streamwise view (total wall clock time = 20 days, computational time 1.25 days for 170 shedding cycles)

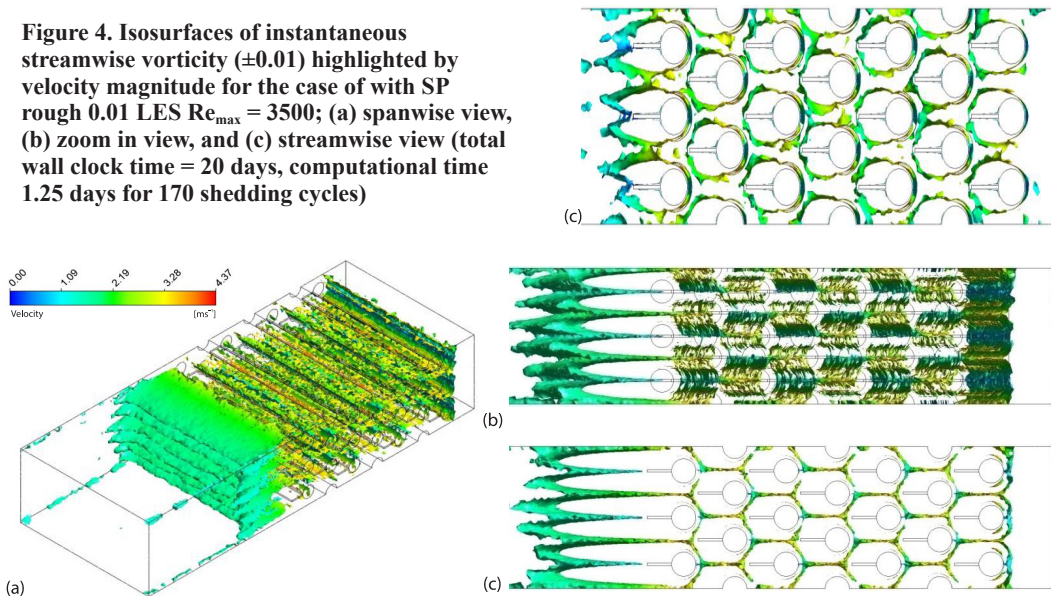


Figure 5. Isosurfaces of instantaneous streamwise vorticity (± 0.01) colored by velocity magnitude for the case of with SP srough 0.01 RANS $Re_{max} = 3500$; (a) spanwise view, (b) streamwise view (b) zoom in view, and (c) streamwise view (total wall clock time = 1.8 days, total computational time 2.75 hrs for 150 iterations)

Local Nusselt number

At the beginning of results discussions from the present work, an interesting point to discuss is the change of the local Nusselt number in a streamwise direction. The designed CFD model enables such a study with the favor of considering seven tube rows in the streamwise direction. The average Nusselt number is calculated from eq. (8) but locally, Nu_x , based on the intermediate temperatures between rows. This is shown in fig. 6 based on all RANS re-

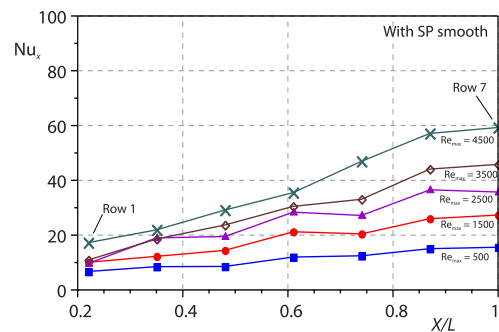


Figure 6. Local Nusselt number for the case of SP smooth

sults, where it is confirmed by the aforementioned knowledge that the, h , stabilizes with little change beyond the fourth or fifth row [4-6]. As shown in fig. 6, at any value of Re_{max} the average Nusselt number value is improved by increasing the turbulence along with the streamwise direction till the fourth or fifth rows. Thereafter, no significant improvement is observed. As an example, at $Re_{max} = 4500$, the Nusselt number improves by about 183% from the 1st row to the 5th row, after that the Nusselt number is slightly changed by 20% till beyond the seventh row. This significant conclusion enhances the credibility of the model utilized in the present study.

Heat transfer rate

The quantity of heat carried beyond the tube bank under specified circumstances is more essential to researchers than the recommended boosting strategy. Figure 7 shows the overall heat transfer rate, Q_a , vs. Re_{max} . The talks use all RANS findings except the six LES points. In fig. 7, the total heat transmitted rises with Re_{max} in all circumstances. The air mass-flow rate decreased the output air temperature. For a shift in Re_{max} from 500-4500, the basal case without SP and homogeneous surfaces improves air heat transmission by 264%. Figure 7 shows that placing SP as extended surfaces enhances heat transfer by 60% throughout the Re_{max} range compared to the basic scenario. Figure 7 shows that increasing heat transfer surface roughness promotes heat transmission. In the baseline scenario (without SP), raising the heat transfer surface irregularity from $k_s/D = 0$ to rugged ($k_s/D = 0.01$) raises the overall heat transfer rate by 15%. However, increasing roughness from 0.01 to 0.02 has minimal effect. In addition adding SP, increasing the surface roughness (k_s/D) irregularity from 0-0.02 raises

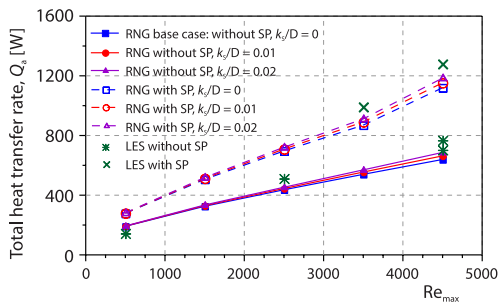


Figure 7. Changing heat transfer rate vs. Re_{max} for all analyzed situations

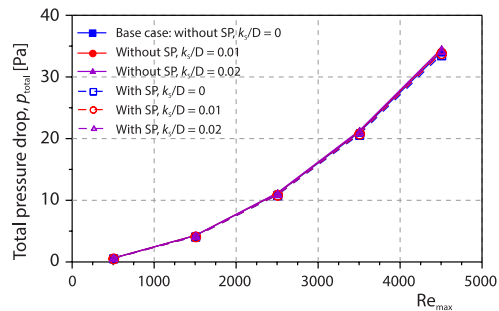


Figure 8. Total pressure drop changes along with Re_{max} for all studied situations

the overall pressure drop of such a heat exchanger by a small amount, adding SP to the basic case reduces it by roughly 2% over the measured Re_{max} range. When different roughness levels

the overall heat transfer rate by 80% across the examined parameter range. Thus, one important finding from the present study showed that the use of roughened surfaces alongside adding SP increases the overall heat transmission rate throughout the Re_{max} 's spectrum. This emphasizes their potential to reduce the energy consumption of industrial heat exchangers and improve their efficiency. The LES data supports these conclusions, while, RANS and LES findings are varied by about 15%.

Pressure drop

Equation 10 illustrates tube bank pressure decrease. Figure 8 illustrates pressure decline vs. Re_{max} for all scenarios examined. Figure 8 shows that increasing \dot{m}_a is the main parameter for improving total tube bank pressure drop, which is reliable with physical explanations and requires greater pumping power. The default pressure drops increase by 349% when the Re_{max} is adjusted from 500-4500 without SP or smooth surfaces. While adding SP as widened surfaces to the trailing ends of tubes reduced

are used, comparable results are obtained. This shows that increased irregularity may be used without fear of increased pressure loss, while heat transmission is improved.

Streamlines, velocity vectors, and turbulent kinetic energy

Figure 9 shows two instances of streamlines and velocity vectors at $Re_{max} = 4500$: fig. 9(a) smooth without SP (base case) and fig. 9(b) rough with SP ($k_s/D = 0.02$). Case (a) Flow topology: upstream flow interacting with the 1st row of tubes causes stagnation patterns. Streamlines in the flow are forced up against the walls of the tube. Because the circumference of the tubes is curved, the separation becomes apparent, and a vortex zone emerges behind them. Streamlines at the conduit's apex and base combine to form a low speed wake re-circulation zone. Prolonging the wake zones to the last row produces expanded velocity zones for the subsequent tube rows. Figure 9(b) shows the flow topology after adding SP to tubes. Pipe-lines with SP have equivalent upstream flow characteristics. The SP change the downstream flow topology. The SP also reduce vortex interference from the top and lower tube walls. The flow streamlines rejoin the SP surfaces from neighboring tubes' borders. Stratified flow with lower vortex amplitude occurs in tubes having SP. The overall tube bank pressure drops and energy losses decrease. This study's comprehensive 3-D simulation without symmetrical borders is similar to previous researchers' flow topology [12, 14].

The impact of flow topology on the enhancement of surface roughness can be attributed to the analysis of turbulent kinetic energy (TKE). The TKE is frequently defined as the measurement of turbulence intensity in fluid-flow [7]. The TKE spreading in the flow field is shown in fig. 10 for two chosen examples at $Re_{max} = 4500$: fig. 10(a) without SP and smooth, and fig. 10(b) with SP and rugged ($k_s/D = 0.02$). In general, fig. 10 shows that the TKE intensity

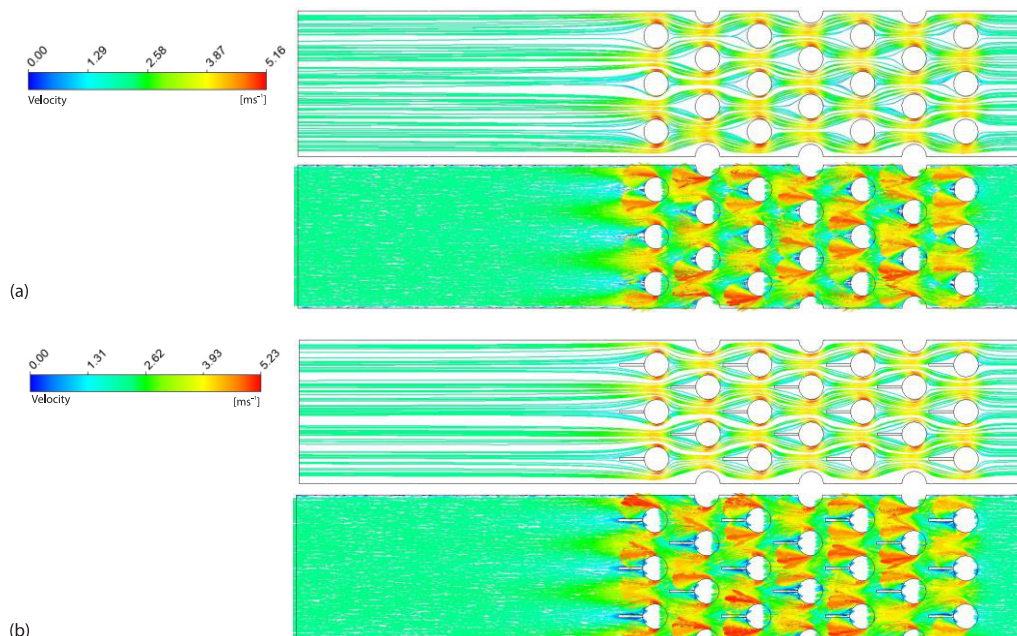


Figure 9. Streamlines and velocity vectors for selected two cases at $Re_{max} = 4500$; (a) base case: without SP, smooth ($k_s/D = 0$) and (b) with SP, rough ($k_s/D = 0.02$)

risers in the streamwise direction and attains its maximum downstream after the last row for all studied situations. Although this rise in TKE for the basic Case (a) smooth without SP is only visible in the last rows, it is considerable. From the second to the final row, the TKE for Scenario (b) with SP and ($k_s/D = 0.02$) grows and is spread equally over the whole configuration. This is partly due to SP ability to prevent vortices from the top and lower tube sides from interacting, resulting in more stratified flow with minor eddies and vortex intensification. As a result, the employment of SP and higher roughens becomes a feasible alternative for enhancing total turbulence inside the tube bank and, as a result, the heat transmitted.

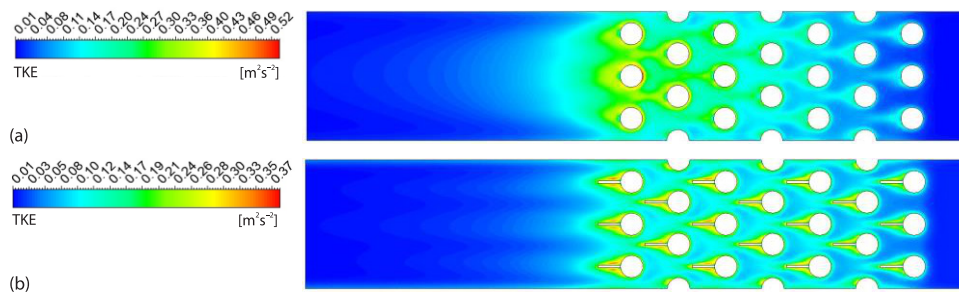


Figure 10. The TKE for chosen two cases at $\text{Re}_{\max} = 4500$;
(a) base case: without SP, smooth ($k_s/D = 0$) and (b) with SP, rough ($k_s/D = 0.02$)

Temperature contours

The importance of exhibiting temperature contours from the current CFD study originates from the fact that temperature variations according to the analyzed scenario resulted in a parameter that determines the improvement of heat transfer rate at a certain air mass-flow rate, or Re_{\max} , eq. (5). Figure 11 shows temperature contours for two examples with $\text{Re}_{\max} = 4500$. The images are created with 100 contours to improve image resolution. The pictures show downstream air temperature rising steadily from the smooth Case (a) to the rough Example (d) ($k_s/D = 0.02$). Unlike instance Case (a), Example (b) bright blue tint is intense, indicating a consistent rise in downstream air temperature. The overall heat transfer enhancement comes from this downstream air temperature gain, which instantly boosts the temperature difference in eq. (5).

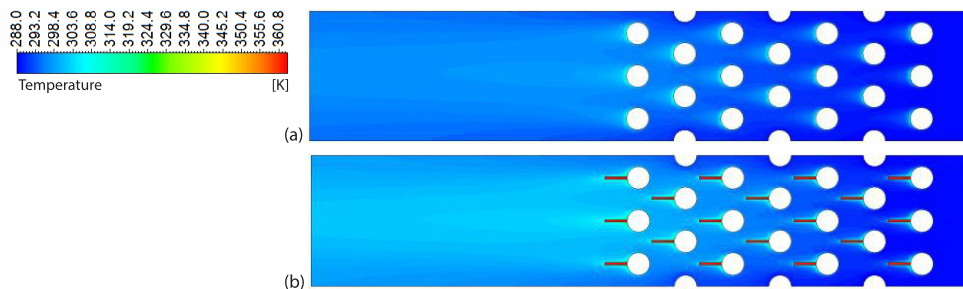


Figure 11. Temperature contours for selected cases at $\text{Re}_{\max} = 4500$;
(a) base case: without SP, smooth ($k_s/D = 0$) and (b) with SP, rough ($k_s/D = 0.02$)

Conclusions

Simulations utilizing comprehensive 3-D RANS and LES methodologies, without the imposition of symmetrical boundary conditions, were conducted to analyze heat transfer

and total pressure drop in a staggered tube bank configuration in cross-flow with air. Providing the option increase the irregularity of the heat transfer surfaces in addition integrating SP to the trailing margins of the tubing. The tube bank of 18 tubes with diameters of 16.4 mm, and longitudinal, transverse, and diagonal pitches of 34.3 mm, 31.3 mm, and 37.7 mm, respectively is investigated. The SP length equals the tube's diameter ($L_{SP}/D = 1$), and the thickness was assumed to be 1.75 mm. Six half-dummy tubes were inserted into the model to maintain the flow characteristics of the staggered configuration. The study's scope was expanded to examine the influence of Re_{max} modifications from 500-4500. While investigating the relative roughness of three surfaces ($k_s/D = 0$ to 0.02) for the two cases with and without SP. All cases were evaluated using the RANS model, but only six examples were designated for the LES model.

A comparative analysis based on the isosurfaces of instantaneous streamwise vorticity, colored by velocity magnitude, was performed to evaluate the performance of LES and RANS models. The findings from the present study highlight the superiority of LES in capturing a broader spectrum of eddies compared to RANS models. However, this advantage comes with the significant drawback of substantially higher computational resource requirements for LES.

Another key observation from the results is that the average local Nusselt number, Nu_x , stabilizes with minimal variation beyond the fourth or fifth row. Furthermore, several additional conclusions can be drawn from the analysis: the total heat transfer rises as Re_{max} rises across all examined scenarios. Additionally, the exit air temperature decreased as the air mass-flow rate rose. The overall heat transfer rate contributed to the air augmented by roughly 264% for a change in Re_{max} from 500-4500 for the case without SP and uniform surfaces (the basal scenario).

Installing SP as extended surfaces significantly enhances the heat transfer rate by roughly 60% across the tested Re_{max} range compared to the base scenario. Additionally, it has been demonstrated that roughening the surfaces of heat transmission enhances the total heat transfer rate. When the effects of surface roughening and the addition of SP are combined, the total heat transfer rate experiences a substantial improvement, highlighting the synergistic effect of these modifications in optimizing thermal performance.

The augmentation in heat transfer surface roughness, coupled with the incorporation of SP, resulted in an impressive nearly 80% enhancement in the total heat transfer rate across the entire spectrum of measured parameters. Notably, increasing surface roughness, as opposed to using SP, was found to further enhance the total heat transfer rate across the examined range of Re_{max} spectrum.

The findings from the LES research are likely to yield similar conclusions, with a notable 15% disparity observed between the results of the RANS and LES models. This discrepancy highlights the potential for further investigation into the underlying causes of turbulence dynamics. Future studies should focus on exploring additional turbulence-enhancing mechanisms to improve model accuracy and further bridge the gap between these two approaches.

The results from the current research, in addition those available in existing literature, offer valuable insights into designing more efficient heat exchangers. These results contribute to enhancing performance and minimizing operational costs in industrial applications, particularly in systems operating at low Reynolds numbers. This improvement has the potential to optimize energy use, increase heat transfer efficiency, and reduce maintenance costs, making it highly relevant for industries seeking cost-effective and sustainable solutions.

Nomenclature

A – area, [m²]
 D – tube outer diameter, [m]
 H – height of fluid duct, [m]
 h – coefficient of convection heat transfer, [Wm⁻²K⁻¹]
 K – thermal conductivity, [Wm⁻¹K⁻¹]
 k_s – height of surface roughness, [m]
 k_s/D – relative roughness, dimensionless
 L – length of SP, [m]
 $LMTD$ – logarithmic mean temperature difference, [K]
 \dot{m} – total air mass-flow rate, [kgs⁻¹]
 Nu – average Nusselt number
 Pr – Prandtl number
 Re – Reynolds number
 p – static pressure, [Pa]
 Q – fluid heat transfer rate, [W]
 S – pitch, [m]
 t – time, [s]
 x – axial advance in the streamwise direction, [m]
 \bar{u}_i – filtered velocity field, [ms⁻¹]
 v – velocity, [ms⁻¹]
 W – width of fluid duct, [m]
 Y^+ – mesh specification near the wall

Acronyms

DNS – direct numerical simulations
 SP – splitter plate
 TKE – turbulent kinetic energy

Greek letters

ρ – density, [kgm⁻³]
 μ – dynamic viscosity, [Pa·s]
 ε – dissipation rate, [m²s⁻³]
 Δ – difference
 τ_{ij} – residual stress tensor

Subscripts

a – air
 avg – average
 D – diagonal
 i – inlet
 L – longitudinal
 max – maximum
 o – outlet
 SP – splitter plate
 s – surface
 T – transversal
 ∞ – upstream fluid

References

- [1] Wang, Y., *et al.*, Study on Characteristics of Fluid-Flow and Heat Transfer in the Torsional Flow Heat Exchanger with Drop-Shaped Tube, *Thermal Science*, 26 (2022), 5A, pp. 3689-3702
- [2] Tacgun, E., Aksoy, I. G., A Numerical Study for Solid and Serrated Annular Finned Tube Bundles, *Thermal Science*, 26 (2022), 6B, pp. 4931-4944
- [3] Djeflal, F., *et al.*, 3-D Assessment of Thermal-Hydraulic Behaviour in Heat Exchangers Fitted by Wavy Annular Fins, *Thermal Science*, 26 (2022), Special Issue 1, pp. S485-S493
- [4] Soundararajan, S., Selvaraj, M., Investigations of Protracted Finned Double Pipe Heat Exchanger System for Waste Heat Recovery from Diesel Engine Exhaust, *Thermal Science*, 27 (2023), 5A, pp. 3783-3793
- [5] Incropera, F., *et al.*, *Fundamentals of Heat and Mass Transfer*, 6th ed., John Wiley and Sons Inc., New York, USA, 2006
- [6] Cengel, Y. A., *Heat Transfer: A Practical Approach*, MacGraw-Hill, New York, USA, 2003
- [7] Wilcox, D. C., *Turbulence Modelling for CFD*, DCW Industries, Inc., 3rd ed., Palm Dr La Canada, Cal., USA, 2006
- [8] Roshko, A., Experiments on the Flow Past a Circular Cylinder at Very High Reynolds Number, *J. Fluid Mech.*, 10 (1961), 3, pp. 345-356
- [9] Apelt, C. J., *et al.*, The Effects of Wake Splitter Plates on the Flow Past a Circular Cylinder in the Range 10000 < Re < 50000, *J. Fluid Mech.*, 61 (1973), 1, pp. 187-198
- [10] Kwon, K., Choi, H., Control of Laminar Vortex Shedding Behind a Circular Cylinder Using Splitter Plates, *Phys. Fluids.*, 8 (1996), 2, pp. 479-486
- [11] Park, W. C., Numerical Investigation of Wake Flow Control by a Splitter Plate, *KSME Int. J.*, 12 (1998), Jan., pp. 123-131
- [12] Mangrulkar, C. K., *et al.*, Experimental and CFD Prediction of Heat Transfer and Friction Factor Characteristics in Cross-Flow Tube Bank with Integral Splitter Plate, *International Journal of Heat and Mass Transfer*, 104 (2017), Jan., pp. 964-978
- [13] Mangrulkar, C. K., *et al.*, Experimental and Numerical Investigations for Effect of Longitudinal Splitter Plate Configuration for Thermal-Hydraulic Performance of Staggered Tube Bank, *International Journal of Heat and Mass Transfer*, 161 (2020), 120280
- [14] Elmekawy, A. M. N., *et al.*, Performance Enhancement for Tube Bank Staggered Configuration Heat Exchanger – CFD Study, Chemical Engineering & Processing, *Process Intensification*, 164 (2021), 108392

- [15] Al-Rubaiy, A., The Effect of Surface Roughness and Free Stream Turbulence on the Flow and Heat Transfer Around a Circular Cylinders, Ph. D. Thesis, University of Sheffield, Sheffield, UK, 2018
- [16] Achenbach, E., Influence of Surface Roughness on the Cross-Flow Around a Circular Cylinder, *Journal of Fluid Mechanics*, 46 (1971), 02, pp. 321-335
- [17] Schultz, M. P., Flack K. A., Turbulent Boundary-layers over Surfaces Smoothed by Sanding, *Journal of Fluid Engineering*, 125 (2003), 5, pp. 863-870
- [18] Arenales, M. R. M., *et al.*, Surface Roughness Variation Effects on Copper Tubes in Pool Boiling of Water, *International Journal of Heat and Mass Transfer*, 151 (2020), 119399
- [19] Bergstrom, D. J., *et al.*, Application of Power Laws to Low Reynolds Number Boundary-Layers on Smooth and Rough Surfaces, *Physics of Fluids*, 13 (2001), 11, pp. 3277-3284
- [20] Gomelauri, V., Influence of 2-D Artificial Roughness on Convective Heat Transfer, *International Journal of Heat and Mass Transfer*, 7 (1964), 6, pp. 653-663
- [21] Krogstadt, P. A., Antonia, R. A., Surface Roughness Effects in Turbulent Boundary-Layers, *Experiments in Fluids*, 27 (1999), 5, pp. 450-460
- [22] Achenbach, E., The Effect of Surface Roughness on the Heat Transfer From a Circular Cylinder to the Cross-flow of Air, *Int. J. Heat Mass Transfer*, 20 (1977), 4, pp. 359-369
- [23] Achenbach, E., Heinecke, E., On Vortex Shedding From Smooth and Rough Cylinders in the Range of Reynolds Numbers 6×10^3 to 5×10^6 , *Journal of Fluid Mechanics*, 109 (1981), Aug., pp. 239-251
- [24] Kolar, V., Heat Transfer in Turbulent Flow of Fluids through Smooth and Rough Tubes, *International Journal of Heat and Mass Transfer*, 8 (1965), 4, pp. 639-653
- [25] Tetsu, F., Influence of Various Surface Roughness on the Natural-Convection, *International Journal of Heat and Mass Transfer*, 16 (1973), 3, pp. 629-636
- [26] Kawamura, T., Takami, H., Computation of High Reynolds Number Flow Around a Circular Cylinder with Surface Roughness, *Fluid Dynamics Research*, 1 (1986), 2, pp. 145-162
- [27] Lakehal, D., Computation of Turbulent Shear Flows over Rough-Walled Circular Cylinders, *Journal of Wind Engineering and Industrial Aerodynamics*, 80 (1999), 1, pp. 47-68
- [28] Dierich, F., Nikrityuk, P. A., A Numerical Study of the Impact of Surface Roughness on Heat and Fluid-Flow Past a Cylindrical Particle, *International Journal of Thermal Sciences*, 65 (2013), Mar., pp. 92-103
- [29] Rodriguez, I., Numerical Simulation of Roughness Effects on the Flow Past a Circular Cylinder, *Journal of Physics: Conference Series*, 745 (2016), 032043
- [30] Chen, N., Influence of Laser-Processed Surfaces on Heat Transfer Performance of Microflow Channels, *Case Studies in Thermal Engineering*, 52 (2023), 103624
- [31] Taylor, J. B., *et al.*, Characterization of the Effect of Surface Roughness and Texture on Fluid-Flow – Past, Present, And Future, *International Journal of Thermal Sciences*, 45 (2006), 10, pp. 962-968
- [32] Karali, M. A., *et al.*, Effect of Surfaces Roughness of a Staggered Tube Bank in Cross-flow with Air on Heat Transfer and Pressure Drop, *Case Studies in Thermal Engineering*, 43 (2023), 102779
- [33] Breuer, M., Large Eddy Simulation of the Subcritical Flow Past a Circular Cylinder: Numerical and Modelling Aspects, *Int. J. Numer. Methods Fluids*, 28 (1998), 9, pp. 1281-1302
- [34] Rodi, W., DNS and LES of Some Engineering Flows, *Fluid Dynamics Research*, 38 (2006), 2-3, pp. 145-173
- [35] Sarkar, S., Large-Eddy Simulation of Wake and Boundary-Layer Interactions Behind a Circular Cylinder, *J. Fluids Eng.*, 131 (2009), 091201
- [36] Afgan, I., *et al.*, Cross-flow over Two Heated Cylinders in Tandem Arrangements at Subcritical Reynolds Number Using Large Eddy Simulations, *Inter. J. of Heat and Fluid-Flow*, 100 (2023), 109115
- [37] Afgan, I., *et al.*, Large Eddy Simulation of the Flow Around Single and Two Side-By-Side Cylinders at Subcritical Reynolds Numbers, *Phys. Fluids*, 23 (2011), 075101
- [38] Abed, N., Afgan, I., A CFD Study of Flow Quantities and Heat Transfer by Changing a Vertical to Diameter Ratio and Horizontal to Diameter Ratio in Inline Tube Banks Using Urans Turbulence Models, *International Communications in Heat and Mass Transfer*, 89 (2017), Dec., pp. 18-30
- [39] Kahil, Y., *et al.*, Simulation of Subcritical-Reynolds-Number Flow Around Four Cylinders in Square Arrangement Configuration Using LES, *European Journal of Mechanics/B Fluids*, 74 (2019), Mar.-Apr., pp. 111-122
- [40] Ibrahim, T. A., Gomaa, A., Thermal Performance Criteria of Elliptic Tube Bundle in Cross-flow, *Int. J. Thermal Science*, 48 (2009), 11, pp. 2148-2158
- [41] Ibrahim, E., Moawed, M., Forced Convection and Entropy Generation from Elliptic Tubes with Longitudinal Fins, *Energy Convers. Manag.*, 50 (2009), 8, pp. 1946-1954

- [42] Ahmed, S. A. E. S., *et al.*, Effect of Longitudinal-External-Fins on Fluid-Flow Characteristics for Wing-Shaped Tubes Bundle in Cross-Flow, *J. Thermodyn.*, 2015 (2015), 542405
- [43] Ahmed, S. S. E., *et al.*, Effect of Attack and Cone Angles on Air-flow Characteristics for Staggered Wing Shaped Tubes Bundle, *Heat Mass Transfer/Waerme – Und Stoffuebertragung*, 51 (2015), 7, pp. 1001-1016
- [44] Nakhchi, M. E., Esfahani, J. A., Numerical Investigation of Turbulent Cuo-Water Nanofluid Inside Heat Exchanger Enhanced with Double V-Cut Twisted Tapes, *J. Therm Anal Calorim*, 145 (2020), May, pp. 2535-2545
- [45] Gorman, J. M., *et al.*, In-Line Tube-Bank Heat Exchangers: Arrays With Various Numbers of Thermally Participating Tubes, *International Journal of Heat and Mass Transfer*, 132 (2019), Apr., pp. 837-847
- [46] Stefanidis, G. D., *et al.*, CFD Simulations of Steam Cracking Furnaces Using Detailed Combustion Mechanisms, *Comput. Chem. Eng.*, 30 (2006), 4, pp. 635-649
- [47] Germano, M., *et al.*, A Dynamic Subgrid-Scale Eddy Viscosity Model, *Phys. Fluids A*, 3 (1991), 7, pp. 1760-1765
- [48] Lilly, D. K., A Proposed Modification of the GermanoSubgrid-Scale Closure Method, *Phys. Fluids A*, 4 (1992), 3, pp. 633-635
- [49] Refaey, H. A., *et al.*, Numerical Investigations of the Convective Heat Transfer from Turbulent Flow over Staggered Tube Bank, *J. Inst. Eng. India Ser., C100* (2019), 6, pp. 983-993
- [50] Hudear, H. R., Shehab, S. N., Cross-Flow Characteristics and Heat Transfer of Staggered Tubes Bundle: a Numerical Study, *Frontiers in Heat and Mass Transfer*, 21 (2023), Nov., pp. 367-383
- [51] Erguvan, M., MacPhee, D. W., Energy and Exergy Analyses of Tube Banks in Waste Heat Recovery Applications, *Energies*, 11 (2018), 2094
- [52] Zhong, Y., *et al.*, Heat Transfer and Flow Resistance in Crossflow over Corrugated Tube Banks, *Energies*, 17 (2024), 1641
- [53] Kusyomov, A. N., *et al.*, Numerical Simulation of 3D Flow over a Circular Cylinder, *J. Phys.: Conf. Ser.*, 2057 (2021), 012072